Journal of Organometallic Chemistry 694 (2009) 3590–3596

Contents lists available at ScienceDirect

Journal of Organometallic Chemistry

journal homepage: www.elsevier.com/locate/jorganchem

Synthesis, spectral and structural characterization of dinuclear rhodium (II) complexes of the anticonvulsant drug valproate with theophylline and caffeine

A. Latif Abuhijleh [a,*], Hijazi Abu Ali [a], Abdul-Hamid Emwas [b]

[a] Department of Chemistry, Birzeit University, P.O. Box 14, West Bank, Palestine
[b] Department of Chemistry and Biochemistry, Miami University, 701 E. High St., Oxford, OH 45056, United States

ARTICLE INFO

Article history:
Received 21 April 2009
Received in revised form 29 June 2009
Accepted 6 July 2009
Available online 23 July 2009

Keywords:
Rhodium (II) valproate
Theophylline
Caffeine
Dinuclear
Bis-adducts
X-ray crystal structure

ABSTRACT

The dinuclear complex tetra(μ-valproato) dirhodium(II), $Rh_2(valp)_4$ (**1**), and its bis-adducts with theophylline, $Rh_2(valp)_4(ThH)_2$ (**4**), or caffeine, $Rh_2(valp)_4(Caf)_2$ (**5**), have been synthesized and characterized by elemental analysis, IR, UV–Vis, magnetic moment, ^1H and ^{13}C NMR spectroscopic techniques. Spectral data for the complexes are consistent with a dinuclear structure as found for rhodium (II) tetracarboxylate adducts. Theophylline and caffeine bases in complexes **4** and **5**, respectively, are axially coordinated to rhodium (II) atoms through the sterically hindered N(9) site. This is confirmed by X-ray crystal structure analyses of complexes **4** and **5**.

1. Introduction

The coordination chemistry of the dinuclear tetracarboxylate complexes of the transition metals are a focus of interest owing to their wide application in many fields, such as material science, catalysis and as anticancer agents [1–8]. Among the compounds that have been investigated as antitumor agents were dirhodium tetracarboxylate complexes. The antitumor activity of these complexes was first discovered by Bear et al. [4,5] and it was found that the activity of dirhodium tetracarboxylate, $Rh_2(OOCR)_4$, to be in the order: methoxyacetate < acetate < propionate < butyrate [5]. The ability of these complexes to function as antitumor agents against many types of tumors, by inhibiting DNA and protein synthesis, has prompted several studies on the nature of rhodium carboxylates formed with various nucleic acids and their constituent bases in order to elucidate their inhibition properties [1,2,8–24]. These investigations have shown that dirhodium tetracarboxylates form stable mono and bis-adducts as well as bridging and/or chelating adducts with a wide variety of ligand types involving donor atoms such as nitrogen, oxygen and sulfur [1,2,8–24]. X-ray crystal structure analyses of tetrakis(-μ-acetato)dirhodium(II) complexes of theophylline and caffeine have shown that in both complexes the dirhodium–tetra-acetate nucleus is occupied at the two axial positions by N(9) of the theophyline and caffeine bases [9].

Valproic acid (2-propylpentanoic acid) $(CH_3CH_2CH_2)_2CHCOOH$, in the form of its sodium salt has a wide spectrum of activity as an anticonvulsant drug [25]. The interaction of this drug with transition metal ions is only known for copper (II) [26]. We prepared several mononuclear and binuclear copper (II) valproate complexes with nitrogen donor ligands and studied their biological activities [27–29]. The present work was undertaken as part of our study of the interaction of the valproate drug with other transition metals. And since the antitumor activity of dirhodium tetracarboxylate may increase with increasing the number of carbon atoms in the carboxylate ion, we extended the interaction of the valproate drug with rhodium (II). We report here the synthesis and spectroscopic characterization of dirhodium (II) tetravalproate and it adducts with theophylline and caffeine and determined crystal structures of these adducts, Scheme 1.

Theophylline (**2**) is chosen as a ligand since it has the same N(7)/O(6) arrangement as guanine. The N(7)/O(6) portion of guanine is the region of DNA which has been discussed in reference to heavy metal–DNA interactions. [9,13,30]. Caffeine (**3**) [where N(7) is blocked] was chosen to compare its coordination site with that of theophylline. In addition, theophylline and caffeine are purine alkaloids possessing several pharmacological properties and their interactions with metals ions gain importance in bioinorganic chemistry.

* Corresponding author. Tel.: +972 2 2982037; fax: +972 2 281 0656.
E-mail address: latif@birzeit.edu (A.L. Abuhijleh).

0022-328X/$ - see front matter © 2009 Elsevier B.V. All rights reserved.
doi:10.1016/j.jorganchem.2009.07.031

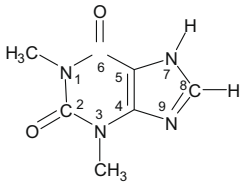
Theophylline, **2**

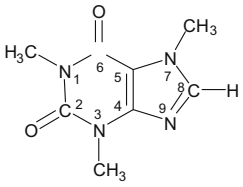
Caffeine, **3**

2. Results and discussion

Results of elemental analyses for the complexes comply with the formula $Rh_2(valp)_4$ or $Rh_2(valp)_4{\cdot}L_2$, when L = theophylline (ThH) or caffeine (Caf). The binary and ternary complexes are soluble in several polar solvents such as diethyl ether (binary complex), chloroform, dichloromethane, acetone, and methanol.

2.1. Infrared spectra

The assignments of IR frequencies for the asymmetrical stretch, $\nu_{asym}(CO_2)$, and the symmetrical stretch, $\nu_{sym}(CO_2)$, of the valproate group are given in Table 1. The $\nu_{asym}(CO_2)$ vibrations for the rhodium valproate and its adducts occur between 1565 and 1585 cm^{-1} and $\nu_{sym}(CO_2)$ vibrations occur at about 1413 cm^{-1}. The values of the difference between $\nu_{asym}(CO_2)$ and $\nu_{sym}(CO_2)$ $\Delta\nu$ = 151–172 cm^{-1}, are consistent with a bidentate bridging mode for the carboxylates [31]. These IR results agree well with those observed in dimeric rhodium complexes of other alkyl carboxylates, [1] in which the carboxylate acts as a "bridging" bidentate ligand. An increase in the $\nu_{asym}(CO_2)$ values for bis-adducts **4** and **5** in comparison to the corresponding value for the binary complex **1** is due to axial coordination of donor base ligands in these adducts [1,2].

In theophylline and caffeine complexes **4** and **5**, respectively, the two C=O (at positions 2 and 6) stretching vibrations of these purines found at about 1710–1712 and 1665–1675 cm^{-1}. This indicates that the exocyclic oxygens at positions 2 and 6 do not participate in coordination since the corresponding vibrations for free purine occurs at about 1712–1718 and 1670–1680 cm^{-1}. Coordination through one of these oxygens may cause a shift to lower energy by about 40–50 cm^{-1} for the carbonyl group of the ligand [32]. The ν(C=N) ring vibration for these free purines occurs at about 1570 cm^{-1} is shifted to lower value at about 1550 cm^{-1} upon the bis-adducts formation may suggest that the coordination of these purines is through imidazole ring.

2.2. Electronic absorption spectra

Electronic absorption spectral data of the complexes in CH_2Cl_2 solutions are given in Table 1. These complexes show two characteristic absorption bands in the visible region. The lower energy

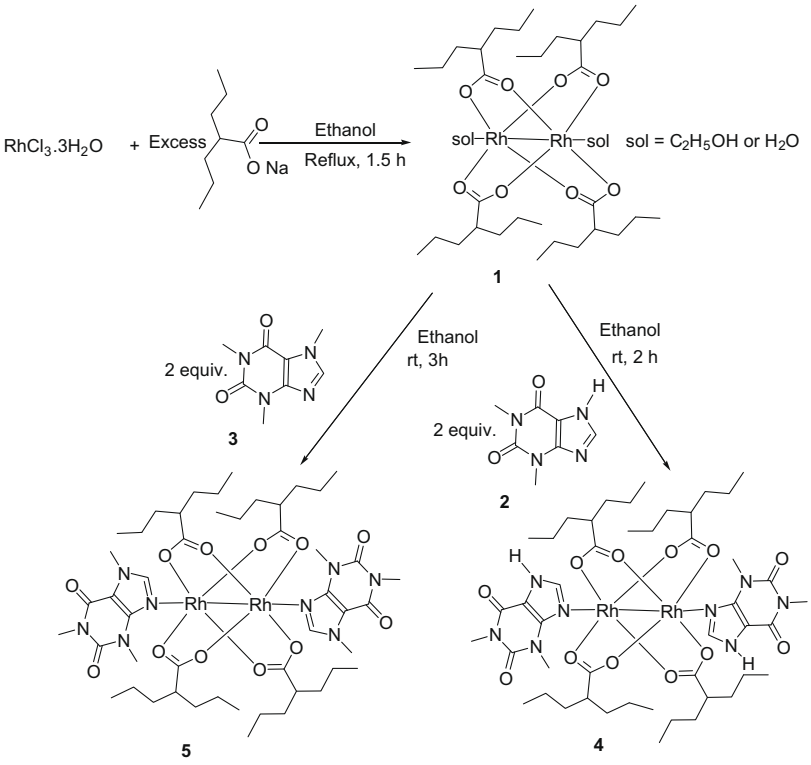

Scheme 1. Syntheses of the complexes **1**, **4** and **5**.

Table 1
Visible and IR spectral data for the complexes.

Compound	λ_{max} (nm) (? = $dm^3\ mol^{-1}\ cm^{-1}$)		ν_{asym} (CO_2) (cm^{-1})	ν_{sym} (CO_2) (cm^{-1})	$\Delta\nu$ (cm^{-1})
	Band I	Band II			
1	612 (250)	442 (110)	1565	1414	151
4	566 (245)	443 (150)	1585	1413	172
5	565 (256)	442 (155)	1582	1413	169

band (**I**) has been assigned as the $\pi^*(RhRh) \rightarrow \sigma^*(RhRh)$ transition and the higher energy band (**II**) as the $\pi^*(RhRh) \rightarrow \sigma^*(Rh–O)$ [1,14,33], or as the $\pi(Rh–O) \rightarrow \sigma^*(Rh–O)$ transition [37]. Band **I** shows blue shift when dirhodium tetracarboxylate complex is coordinated to a stronger axial ligand compared with the absorption peak of $Rh_2(O_2CCR)_4$ without any axial ligands [33]. In addition, the nature of the axial ligand defines the apparent color of the adduct. The adducts formed are green or blue-green for oxygen donor ligands, rose-red, violet, purple or pink for nitrogen donors, and violet, purple, or orange for sulfur donors [35]. The purple or violet color and the shift of the absorption peak of band **I** to higher energy for the bis-adducts **4** and **5** compared with the absorption peak of the binary $Rh_2(valp)_4$ complex (Table 1) is in agreement with an axial nitrogen donor ligands [1,14]. Band **II** in the visible region of dirhodium tetracarboxylates does not depend on the nature of axial ligands but it depends on the nature of the equatorial ligands, i.e. the nature of the carboxylate group [1]. For the complexes under investigation, the energy of this band remains essentially constant (Table 1) around 442 nm. These spectral results are consistent with the presence of four bridging valproate groups in equatorial positions of dirhodium (II) atoms in the binary and ternary adducts, while the nitrogen donor ligands are occupying the axial positions in the ternary bis-adducts with theophylline or caffeine.

2.3. Magnetic moment

The magnetic moments (μ_{eff}), which were calculated from the magnetic susceptibilities, are those for diamagnetic compounds. They are in the same range of other dinuclear rhodium (II) carboxylates having $\sigma^2 \pi^4 \delta^2 \pi^{*4} \delta^{*2}$ electronic configuration with a single bond between the two rhodium (II) atoms, such as the well-known rhodium (II) acetate and its bis-adducts [1], indicating the existence of the same dinuclear structure in the present rhodium (II) valproate complexes. The two rhodium (II) atoms are bridged by four valproate groups, without donor base ligands in the axial positions, compound **1**, or the axial positions are occupied by purine molecules, compounds **4** and **5**.

2.4. ^1H and ^{13}C Nuclear magnetic resonance

Proton NMR spectrum of $Rh_2(valp)_4$ in $CDCl_3$ shows triplet of CH_3 groups centered at 0.70 ppm, sixtet centered at 1.0 ppm of CH_2 groups next to the CH_3 groups, complex signals at about 1.10 ppm and at 1.25 due to CH_2 groups attached to CH, and complex signal at about 1.98 ppm of CH proton, having an intergration ratio 6:4:2:2:1. The corresponding valproate proton signals of the bis-adducts of caffeine or theophylline obtained in $CDCl_3$ occur at about 0.8, 1.1, 1.2, 1.35 and 2.1 ppm having an integration ratio 6:4:2:2:1. The results of the integrated spectrum of each of these adducts indicated also that there are two molecules of caffeine or theophylline per tetra (μ-valproato) dirhodium (II) unit. This is consistent with the analytical results in showing that rhodium (II) valproate dimer forms bis-adducts in which two purine ligands are occupying both axial positions.

Several coordination sites are available in theophylline and caffeine to bind metal ions. In addition to the nitrogen donor atoms, and to carbonyl oxygens, it has been recently shown that these purine bases can bind through C(8) atom [36]. To determine the coordination site of theophylline and caffeine in complexes **4** and **5**, respectively, ^1H and ^{13}C NMR ($CDCl_3$) spectra of these complexes are obtained and compared with those obtained for the parent purine ligands and the results are summarized in the Section 4. ^1H

Table 2
^{13}C NMR ($CDCl_3$) chemical shifts (ppm).

Compound	N_1–CH_3	N_3–CH_3	N_7–CH_3	C_2	C_4	C_5	C_6	C_8
ThH (**2**)	28.53	30.28	–	151.58	149.06	106.93	156.24	140.30
$Rh_2(valp)_4(ThH)_2$ (**4**)	29.05	31.60	–	152.15	150.07	108.11	156.98	144.76
$\Delta\delta$	0.52	1.32	–	0.57	1.01	1.18	0.74	4.46
Caf (**3**)	27.94	29.76	33.60	151.75	148.75	107.63	155.46	141.41
$Rh_2(valp)_4(Caf)_2$ (**5**)	28.20	30.71	34.10	152.01	149.35	108.34	155.58	145.14
$\Delta\delta$	0.26	0.95	0.50	0.27	0.60	0.71	0.12	3.13

$\Delta\delta$ is the chemical shift difference between coordinated ligand to rhodium and free ligand.

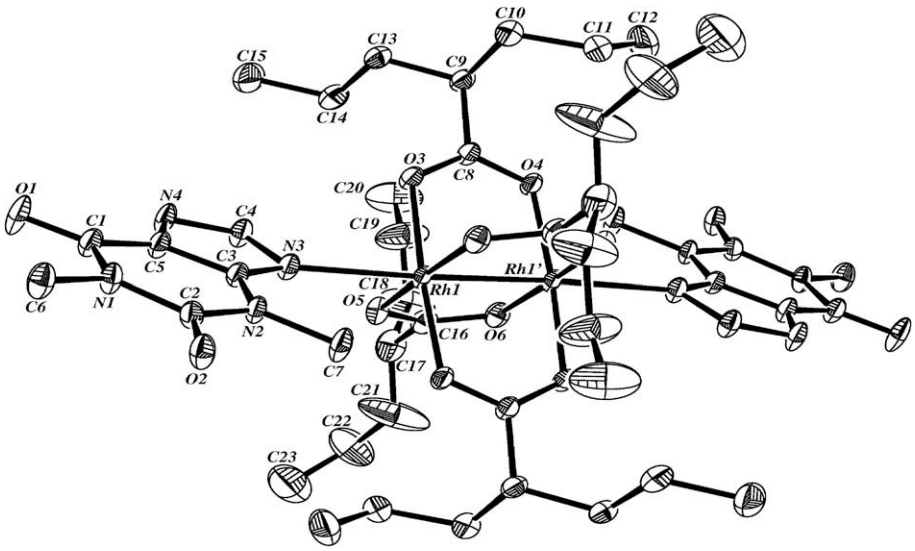

Fig. 1. View of the molecular structure of **4**, showing the atom numbering scheme. Ellipsoids represent thermal displacement parameters at the 30% probability level.

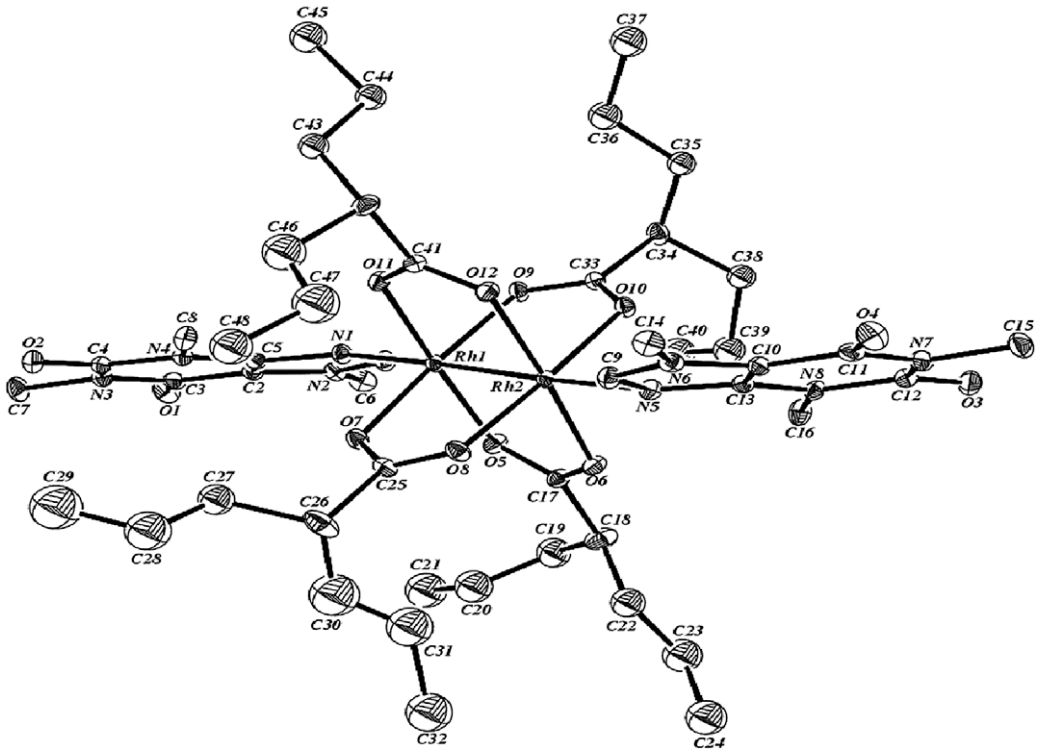

Fig. 2. View of the molecular structure of **5**, showing the atom numbering scheme. Ellipsoids represent thermal displacement parameters at the 50% probability level.

NMR ($CDCl_3$) spectra for complexes **4** and **5** exhibit downfield shifts relative to the corresponding parent purine protons. For complex **4**, $\Delta\delta$ 0.12 N(1)–CH_3, 0.38 N(3)–CH_3, 1.00 C(7)–H, 0.46 C(8)–H. Complex **5**, $\Delta\delta$ 0.12 N(1)–CH_3, 0.41 N(3)–CH_3, 0.13 N(7)–CH_3, 0.49 C(8)–H, see Section 4 and Table 2.

The highest proton shifts for complexes **4** and **5** are those of C(8)–H and N(3)–CH_3. ^{13}C NMR spectra for these bis-adducts show that all carbon resonances for the purine ligands in these adducts are downfield shifted relative to the corresponding resonances of the parent purine. For complex **4**, $\Delta\delta$ 0.52 ($N1CH_3$), 1.32 ($N3CH_3$), 1.18 (C5), 4.46 (C8), 1.01 (C4), 0.57 (C2), 0.74 (C6). For complex **5**, $\Delta\delta$ 0.26 ($N1CH_3$), 0.95 ($N3CH_3$), 0.50 ($N7CH_3$), 0.71 (C5), 3.13 (C8), 0.60 (C4), 0.27 (C2), 0.12 (C6), Section 4. An inspection of these data indicate that the highest shifts are those for C(8) and CH_3 carbon of N(3)–CH_3. These ^1H and ^{13}C results indicate that theophylline or caffeine molecules in complexes **4** and **5**, respectively, bind to $Rh_2(valp)_4$ core through N(9). It is well-known that upon metal coordination to purine ring nitrogen atoms, extensive π-electron redistribution of the ring occurs, causing the protons and carbons adjacent to the binding site more acidic and, thus, experience downfield chemical shifts [12]. The axial coordination of two theophylline or caffeine molecules through N(9) to $Rh_2(valp)_4$ core in solid state is confirmed by X-ray crystal structure determination of the complexes **4** and **5**, respectively.

Table 3
Selected bond distances (Å) and angles (°) for **4**.

O(1)–C(1)	1.227(4)	C(8)–O(3)–Rh(1)	118.2(2)
C(1)–N(1)	1.398(4)	C(8)–O(4)–Rh(1)#1	119.7(2)
C(1)–C(5)	1.406(5)	C(16)–O(5)–Rh(1)	119.2(2)
C(2)–N(2)	1.368(4)	C(16)–O(6)–Rh(1)#1	119.4(2)
C(3)–N(3)	1.360(4)	O(3)–Rh(1)–O(6)#1	88.78(10)
C(8)–O(4)	1.261(4)	O(3)–Rh(1)–O(4)#1	175.78(9)
C(11)–C(12)	1.495(7)	O(6)#1–Rh(1)–O(4)#1	89.79(10)
C(16)–O(5)	1.264(4)	O(3)–Rh(1)–O(5)	90.22(10)
C(16)–C(17)	1.515(6)	O(6)#1–Rh(1)–O(5)	176.02(9)
N(3)–Rh(1)	2.303(3)	O(4)#1–Rh(1)–O(5)	90.94(10)
N(7)–Rh(2)	2.309(3)	O(3)–Rh(1)–N(3)	87.07(10)
O(3)–Rh(1)	2.029(2)	O(6)#1–Rh(1)–N(3)	94.96(10)
O(4)–Rh(1)#1	2.036(2)	O(4)#1–Rh(1)–N(3)	97.00(9)
O(5)–Rh(1)	2.042(2)	O(5)–Rh(1)–N(3)	88.84(10)
O(10)–Rh(2)#2	2.028(3)	O(3)–Rh(1)–Rh(1)#1	88.83(7)
O(11)–Rh(2)	2.037(3)	O(6)#1–Rh(1)–Rh(1)#1	88.06(7)
Rh(2)–O(12)#2	2.031(3)	O(4)#1–Rh(1)–Rh(1)#1	87.16(6)
Rh(1)–Rh(1)#1	2.3926(5)	O(5)–Rh(1)–Rh(1)#1	88.07(7)
Rh(2)–Rh(2)#2	2.3936(7)	N(3)–Rh(1)–Rh(1)#1	174.85(7)

Table 4
Selected bond distances (Å) and angles (°) for **5**.

C(4)–O(2)	1.200(8)	O(8)–C(25)–O(7)	126.3(6)
C(4)–N(4)	1.390(8)	O(7)–C(25)–C(26)	116.0(7)
C(5)–N(4)	1.363(8)	O(11)–C(41)–C(42)	118.2(6)
C(6)–N(2)	1.456(8)	O(12)–C(41)–C(42)	115.6(6)
C(7)–N(3)	1.469(8)	C(43)–C(42)–C(41)	115.8(7)
C(25)–O(7)	1.286(8)	C(25)–O(7)–Rh(1)	119.1(4)
C(25)–C(26)	1.511(10)	C(25)–O(8)–Rh(2)	118.2(4)
C(27)–C(28)	1.393(16)	C(41)–O(11)–Rh(1)	119.0(4)
C(41)–O(12)	1.262(7)	C(41)–O(12)–Rh(2)	118.8(4)
C(41)–C(42)	1.528(9)	O(5)–Rh(1)–O(11)	176.07(17)
C(42)–C(46)	1.657(15)	O(7)–Rh(1)–O(11)	90.59(18)
C(43)–C(44)	1.476(11)	O(7)–Rh(1)–N(1)	94.81(18)
N(1)–Rh(1)	2.325(5)	O(11)–Rh(1)–N(1)	97.71(18)
N(5)–Rh(2)	2.324(5)	O(9)–Rh(1)–N(1)	89.05(17)
O(6)–Rh(2)	2.050(4)	O(5)–Rh(1)–Rh(2)	88.28(12)
O(7)–Rh(1)	2.031(4)	O(7)–Rh(1)–Rh(2)	87.54(12)
O(8)–Rh(2)	2.042(4)	O(11)–Rh(1)–Rh(2)	87.79(12)
O(9)–Rh(1)	2.046(4)	O(9)–Rh(1)–Rh(2)	88.44(11)
O(10)–Rh(2)	2.043(4)	N(1)–Rh(1)–Rh(2)	173.99(14)
O(11)–Rh(1)	2.035(4)	O(12)–Rh(2)–Rh(1)	88.05(12)
Rh(1)–Rh(2)	2.3956(6)	N(5)–Rh(2)–Rh(1)	175.44(13)

2.5. X-ray crystal structure determination of the complexes **4** and **5**

View of the molecular structures for **4**, and **5** with numbering scheme are shown in Figs. 1 and 2, respectively. Selected bond

distances and angles for the complexes are reported in Tables 3 and 4. The Rh(II) atoms in structures **4** and **5** are bridged by carboxylate groups that span an average metal–metal bond distance of 2.3936(7) and 2.3956(7) Å, respectively, which is very similar to those of many dirhodium compounds [19]. Octahedral coordination at Rh in complex **4** is completed by theophylline moiety bound axially *via* the unprotected N(9) nitrogen atom and by caffeine in complex **5** also *via* the unprotected N(9) nitrogen atom. The Rh–N bond distances in compound **4**, 2.309(3) and 2.303(3), and 2.324(5) and 2.325(5) in **5** are larger than [dirhodium (acetato)$_4$ (theophyline)$_2$] complexes, 2.230(3), [dirhodium (acetato)$_4$ (caffeine)$_2$] complexes, 2.315(9) [9] and dirhodium bipyridine (bpy) compounds, 2.224(2) and 2.264(2) [19,23,34] and almost similar to other dirhodium complexes [23]. The difference between Rh–N bond lengths in these complexes may be attributed to steric hindrance between the axial ligands and the substituted carboxylate groups; i.e. valproate is larger than the acetate ions. On the other hand, the difference in the Rh–N bond distance between (**4** and **5**) and dirhodium bpy compounds may be attributed to the different binding modes of **4** and **5**, monodentate versus bidentate in dirhodium bpy compounds and other bidentate N-ligands. As expected, the two axial Rh–N bonds are much longer than the average Rh(1)–O and Rh(2)–O equatorial bonds{2.035(4) Å}. The *eq* Rh–O bond distances are very similar to those of other dirhodium carboxylate compounds [19,23,34]. The average bonding angles deviate slightly from those of an ideal octahedron [23].

3. Conclusion

Dirhodium tetravalproate $Rh_2(valp)_4$ interacts with theopylline and caffeine to form the bis-adducts $Rh_2(valp)_4{\cdot}L_2$. X-ray structural analyses for these adducts showed that they are dimers with four bridging carboxylates of the valproate ions between the two rhodium atoms and two N-purine ligands in the axial trans positions with respect to the Rh–Rh bond. The Rh–Rh bond distances are in the range expected for dirhodium tetracarboxylate complexes [19]. The axial Rh–N bond distances in these adducts are longer than, the corresponding bond distance in dirhodium tetraacetate bis-adducts with these purines [9]. This is attributed to steric hindrance between the axial ligands and larger substituted alkyl carboxylate in valproate compare to the acetate. The axial coordination through sterically hindered N(9) atom rather than the preferred N(7) coordination site in theophylline (N(7) is blocked in caffeine) may be attributed to electrostatic repulsion between the exocyclic carbonyl oxygen O(6) of theophylline and the carboxylate oxygen atoms of the valproate ligands [8,9]. If the N(9) coordination site is blocked as in guanine and polyguanylic acid, these DNA nucleobases are not expected to interact with dirhodium tetracarboxylates in the axial positions. It was reported the guanine reacts with $Rh_2(O_2CCH_3)_4(MeOH)_2$ by displacing one or two equatorial acetate ligands to produce equatorially N(7)/O(6) guanine bridging complexes [8,13,22]. The interaction of $Rh_2(valp)_4$ with other purine bases and their corresponding nucleosides and nucleotides are being investigated and the results will be reported in due course.

4. Experimental

4.1. Materials

Rhodium (III) chloride trihydrate, $RhCl_3{\cdot}3H_2O$, sodium valproate, caffeine, theophylline, were from Sigma and $CDCl_3$ was from Aldrich.

4.2. Synthesis

4.2.1. Synthesis of tetra (μ-valproato) dirhodium (II), $Rh_2(valp)_4$ (**1**)

1.0 g of $RhCl_3.3H_2O$ was dissolved in 50 ml of absolute ethanol and saturated with sodium valproate. The resulting brick-red solution was refluxed for 1.5 h. The dark-green solution which formed was cooled to room temperature and filtered to remove the excess sodium valproate, the green filtrate was left in the hood to evaporate. The green precipitate that formed was washed with water and dried *in vacuo* at about 110 °C. ^{1}H NMR ($CDCl_3$): δ 0.70 (t, 6H, CH_3, $^3J_{H-H}$ = 6.9 Hz), 1.00 (sixt, 4H, CH_2, $^3J_{H-H}$ = 7.1 Hz), 1.10–1.25 (m, 4H, CH_2), 1.98 (m, 1H, CH). Anal. Calc. for $C_{32}H_{60}O_8Rh_2$: C, 49.37; H, 7.71. Found: C, 49.55; H, 7.82%.

4.2.2. Synthesis of bis(theophylline)tetra(μ-valproato)dirhodium(II), $Rh_2(valp)_4(ThH)_2$ (**4**)

$Rh_2(valp)_4$ (0.10 g, 0.13 mmol) and theophylline (0.047 g, 0.26 mmol) were stirred together at room temperature in absolute ethanol (15 ml) for 2 h. The blue solution was filtered and left in the hood to evaporate. The violet precipitate that formed was recrystallized from acetone to produce crystals suitable for X-ray measurements. ^{1}H NMR ($CDCl_3$): δ 0.80 (t, 6H, CH_3, $^3J_{H-H}$ = 6.9 Hz), 1.10 (sixt, 4H, CH_2, $^3J_{H-H}$ = 7.1 Hz), 1.20–1.35 (m, 4H, CH_2), 2.10 (m, 1H, CH), 8.30 (s, purine H(8)). ^{13}C{^{1}H} NMR ($CDCl_3$): δ 29.05 (N1CH_3), 31.60 (N3CH_3), 108.11 (C5), 144.76 (C8), 150.07 (C4), 152.15 (C2), 156.98 (C6). Anal. Calc. for $C_{46}H_{76}N_8O_{12}Rh_2$: C, 48.51; H, 6.68; N, 9.84. Found: C, 48.35: H, 6.55: N, 9.65%.

4.2.3. Synthesis of bis(caffeine)tetra(μ-valproato)dirhodium(II), $Rh_2(valp)_4(Caf)_2$ (**5**)

$Rh_2(valp)_4$ (0.10 g, 0.13 mmol) and caffeine (0.05 g, 0.26 mmol) were stirred together at room temperature in absolute ethanol (15 ml). The initial green solution rapidly became purple which was stirred for 3 h. The dark purple precipitate that formed was recrystallized from acetone to produce crystals suitable for X-ray measurements. ^{1}H NMR ($CDCl_3$): δ 0.80 (t, 6H, CH_3, $^3J_{H-H}$ = 6.9 Hz), 1.10 (sixt, 4H, CH_2, $^3J_{H-H}$ = 7.1 Hz), 1.20–1.35 (m, 4H, CH_2), 2.10 (m, 1H, CH), 7.90 (s, purine H(8)). ^{13}C{^{1}H} NMR ($CDCl_3$): δ 28.20 (N1CH_3), 30.71 (N3CH_3), 34.71 (N7CH_3), 108.34 (C5), 145.14 (C8), 149.35 (C4), 152.01 (C2), 155.58 (C6). Anal. Calc. for $C_{48}H_{80}N_8O_{12}Rh_2$: C, 49.40; H, 6.86; N, 9.61. Found: C, 49.27; H, 6.71; N, 9.48%.

4.3. Physical measurements

Elemental analyses for C, H and N were performed by Galbraith Laboratories, Knoxville, TN, USA. Electronic spectra of dichloromethane solutions were obtained with a Hewlett Pickard 8453 diode array spectrophotometer. IR spectral of Nujol mulls sealed between polyethylene sheets were obtained in the 4000 to 200 cm^{-1} region with a Perkin–Elmer model 843 IR spectrophotometer. ^{1}H and ^{13}C NMR measurements of the complexes in deuterated chloroform solutions were carried out at 298 K on a 600 MHz Bruker spectrometer. Chemical shifts were referenced to $SiMe_4$. Magnetic susceptibilities at room temperature were measured by the Gouy method.

4.3.1. X-ray crystallography

Single crystals suitable for X-ray measurements of the complexes **4** and **5** were attached to a glass fiber, with epoxy glue, and transferred to a Bruker SMART APEX CCD X-ray diffractometer system controlled by a Pentium-based PC running the SMART software package, [37] The crystal was mounted on the three-circle goniometer with χ fixed at +54.76°. The diffracted graphite-monochromated Mo Kα radiation (λ = 0.71073 Å) was detected on a phosphor screen held at a distance of 6.0 cm from the crystal oper-

Table 5
Crystal data and structure refinement for **4** and **5**.

	4	**5**
Formula	$C_{46}H_{76}N_8O_{12}Rh_2$	$C_{48}H_{80}N_8O_{12}Rh_2$
Formula weight	1138.97	1167.02
Temperature (*K*)	173(1)	295(1)
Radiation	Mo Kα, 0.71073 Å	Mo Kα, 0.71073 Å
Crystal size (mm^3)	0.37 × 0.22 × 0.09	0.19 × 0.18 × 0.16
crystal system	triclinic	triclinic
Space group	$P\bar{1}$	$P\bar{1}$
a (Å)	12.3126(16)	13.6302(9)
b (Å)	13.2463(18)	18.0972(11)
c (Å)	18.247(3)	23.2958(15)
α (°)	72.108(2).	97.8940(10)
β (°)	73.264(2)	93.1610(10)
λ (°)	73.048(2).	102.8210(10).
V ($Å^3$)	2643.9(6)	5528.1(6)
Z	2	4
d_{calc} ($g\,cm^{-3}$)	1.431	1.402
F(0 0 0)	2440	2440
μ (mm^{-1})	0.689	0.661
θ range (°)	1.77–26.00	1.57–27.00
Reflections collected	27 885	56 379
Independent reflections	10 340 [R_{int} = 0.0359]	23 707 [R_{int} = 0.0607]
h k l limits	−15, 15/−16, 16/−22, 22	−17, 17/−22, 23/−29, 29
Completeness to theta = 27.00°	99.4%	98.2%
Absorption correction	integration	none
Maximum and minimum transmission	0.9406 and 0.7847	0.9017 and 0.8848
Refinement method	full-matrix least-squares on F^2	full-matrix least-squares on F^2
Data/restraints/parameters	10 340/0/633	23 707/0/1049
Goodness-of-fit on F^2	1.047	0.937
Final *R* indices[a] [I>2sigma(I)]	R_1 = 0.0482, wR_2 = 0.1128	R_1 = 0.0703, wR_2 = 0.1635
R indices (all data)	R_1 = 0.0582, wR_2 = 0.1181	R_1 = 0.1267, wR_2 = 0.1840
Largest difference peak and hole (e $Å^{-3}$)	1.018 and −0.663	1.373 and −0.748

[a] $R_1 = \sum||F_o| - |F_c||/\sum F_o$ and $wR_2 = \{\sum[w(F_o^2 - F_c^2)2]/[w(F_o^2)2]\}^{1/2}$.

ating at −43 °C. A detector array of 512 × 512 pixels, with a pixel size of approximately 120 μm, was employed for data collection. The detector centroid and crystal-to-detector distance were calibrated from a least-squares analysis of the unit cell parameters of a carefully centered YLID reference crystal.

After the crystal of the complex had been carefully optically centered within the X-ray beam, a series of 30 data frames measured at 0.3° increments of ω were collected with three different 2θ and φ values to assess the overall crystal quality and to calculate a preliminary unit cell. For the collection of the intensity data, the detector was positioned at a 2θ value of −28° and the intensity images were measured at 0.3° intervals of ω for duration of 20 s. each. The data frames were collected in four distinct shells which, when combined, measured more than 1.3 hemispheres of intensity data with a maximum 2θ of 46.5°. Immediately after collection, the raw data frames were transferred to a second PC computer for integration by the SAINT program package [38]. The background frame information was updated according to the equation $B' = (7B + C)/8$, where B' is the update pixel value, B is the background pixel value before updating, and C is the pixel value in the current frame. The integration was also corrected for spatial distortion induced by the detector. In addition, pixels that reside outside the detector active area or behind the beam stop were masked during frame integration. The integrated intensities for the four shells of data were merged to one reflection file. The data file was filtered to reject outlier reflections. The rejection of a reflection was based on the disagreement between the intensity of the reflection and the average intensity of the symmetry equivalents to which the reflection belongs. In the case of strong reflections ($I > 99\sigma(I)$) which contains only two equivalents, the larger of the two equivalents was retains. The structure was solved and refined by the SHELXTL software package [39].

Crystal data and more details of the data collections and refinements are summarized in Table 5.

Appendix A. Supplementary material

CDC 724336 and 724335 contains the supplementary crystallographic data for **4** and **5**. These data can be obtained free of charge from The Cambridge Crystallographic Data Centre via www.ccdc.cam.ac.uk/data_request/cif.

Supplementary data associated with this article can be found, in the online version, at doi:10.1016/j.jorganchem.2009.07.031.

References

[1] E.B. Boyar, S.D. Robinson, Coord. Chem. Rev. 50 (1983) 109.
[2] H.T. Chifotides, K.R. Dunbar, Rhodium compounds, in: F.A. Cotton, C. Murillo, R.A. Walton (Eds.), Multiple Bonds between Metal Atoms, third ed., Springer Science and Business Media Inc., New York, 2005, pp. 465–589 (Chapter 12) and references therein.
[3] D.J. Timmons, M.P. Doyle, Chiral dirhodium(II) catalyst and their applications, in: F.A. Cotton, C. Murillo, R.A. Walton (Eds.), Multiple Bonds between Metal Atoms, third ed., Springer Science and Business Media Inc., New York, 2005, pp. 591–632 (Chapter 13).
[4] R.G. Hughes, J.L. Bear, A.P. Kimball, Proc. Am. Assoc. Cancer Res. 13 (1972) 120.
[5] R.A. Howard, A.P. Kimball, J.L. Bear, Cancer Res. 39 (1979) 2568.
[6] B.K. Keppler, M. Henn, U.M. Juhl, M.R. Berger, R.E. Biebl, F.E. Wagner, Prog. Clin. Biochem. Med. 10 (1989) 41.
[7] B.K. Keppler, New J. Chem. 14 (1990) 389.
[8] H.T. Chifotides, K.R. Dunbar, Acc. Chem. Res. 38 (2005) 146. and references therein.
[9] K. Aoki, H. Yamazaki, J. Chem. Soc., Chem. Commun. (1980) 186.
[10] T.M. Dyson, E.C. Morrison, D.A. Tocher, L.D. Dale, D.I. Edwards, Inorg. Chim. Acta 169 (1990) 127.
[11] J.R. Rubin, T.P. Haromy, M. Sundaralingam, Acta Crystallogr. C47 (1991) 1712.
[12] H.T. Chifotides, K.R. Dunbar, J.H. Matonic, N. Katsaros, Inorg. Chem. 31 (1992) 4628. and references therein.
[13] K.R. Dunbar, J.H. Matonic, V.P. Saharan, C.A. Crawford, G. Christou, J. Am. Chem. Soc. 116 (1994) 2201.
[14] H. Kitamura, T. Ozawa, K. Jitsukawa, H. Masuda, Y. Aoyama, H. Einaga, Inorg. Chem. 39 (2000) 3294.
[15] N.N. Sueshnikov, M.H. Dickman, M.T. Pope, Acta Crystallogr. (2000) 1193.
[16] S. Rockitt, R. Wartchow, Ho Duddeck, A. Drabczynska, K.K. Kononwicz, Z. Naturforsch 56b (2001) 319.
[17] W.M. Xue, F.E. Kuhn, Eur. J. Inorg. Chem. (2001) 2041.

[18] K. Aoki, M.A. Salam, Inorg. Chim. Acta 339 (2002) 427.
[19] H.T. Chifotides, J.S. Hess, A.M. A Boza, J.R.G. Mascaros, K. Sorasaenee, K.R. Dunbar, Dalton Trans. (2003) 4426.
[20] M.S. Nothenberg, A.R. de Souza, J.doR. Matos, Polyhedron 19 (2000) 1305.
[21] P.M. Bradley, A.M.A. Boza, K.R. Dunbar, C. Turro, Inorg. Chem. 43 (2004) 2450.
[22] (a) H.T. Chifotides, K.M. Koshlap, L.M. Perez, K.R. Dunbar, J. Am. Chem. Soc. 125 (2003) 10703;
(b) H.T. Chifotides, K.M. Koshlap, L.M. Perez, K.R. Dunbar, J. Am. Chem. Soc. 125 (2003) 10714.
[23] A.A. Sidorov, G.G. Aleksandrov, E.V. Pakhmutova, A.Y. Chernyader, I.L. Eremenko, I.I. Moiseer, Russ. Chem. Bull., Inter. Ed. 54 (2005) 588.
[24] A. R de Souza, E.P. Coelho, S.B. Zyngier, Eur. J. Med. Chem. 41 (2006) 1214.
[25] A.G. Chapman, P.E. Keane, B.S. Meldrum, J. Simiand, J.C. Vernieres, Prog. Neurobiol. 19 (1982) 315.
[26] C.C. Hadjikostas, G.A. Katsoulos, M.P. Sigalas, C.A. Tsipis, J. Mrozinski, Inorg. Chim. Acta 167 (1990) 165.
[27] A.L. Abuhijleh, C. Woods, Inorg. Chim. Acta 209 (1993) 187.
[28] A.L. Abuhijleh, C. Woods, J. Inorg. Biochem. 64 (1996) 55.
[29] A.L. Abuhijleh, J. Inorg. Biochem. 68 (1997) 167.
[30] D. Cozak, A. Mardhy, M.J. Oliver, A.L. Beauchamp, Inorg. Chem. 25 (1986) 2600.
[31] K. Nakamoto, Infrared and Raman Spectra of Inorganic and Coordination Compounds, fourth ed., Wiley Interscience, New York, 1986.
[32] G. Pneumatikakis, A. Yannopoulos, J. Markopoulos, C. Angelopoulos, Inorg. Chim. Acta 152 (1998) 101.
[33] T. Kawamura, H. Katayama, H. Nishikawa, T. Yamabe, J. Am. Chem. Soc. 111 (1989) 8156.
[34] J.W. Trexler Jr., A.F. Schreiner, F.A. Cotton, Inorg. Chem. 27 (1988) 3265.
[35] L. Rainen, R.A. Howard, A.P. Kimball, J .L. Bear, Inorg. Chem. 14 (1976) 2752. and references therein.
[36] L.G.F. Lopes, A. Wieraszko, Y. El-Sherif, M.J. Clarke, Inorg. Chim. Acta 312 (2001) 15. and references therein.
[37] SMART-NT V5.6, Bruker AXS GMBH, D-76181 Karlsruhe, Germany, 2002.
[38] SAINT-NT V5.0, Bruker AXS GMBH, D-76181 Karlsruhe, Germany, 2002.
[39] SHELXTL-NT V6.1, Bruker AXS GMBH, D-76181 Karlsruhe, Germany, 2002.